Int. J. Solids Structures, 1977, Vol. 13, pp. 1141–1155. Pergamon Press. Printed in Great Britain

FINITE STRIP BUCKLING ANALYSIS OF CURVED PLATE ASSEMBLIES UNDER BIAXIAL LOADING

D. J. DAWE
Department of Civil Engineering, University of Birmingham, Birmingham, England

(*Received* 28 *September* 1976; *revised* 6 *May* 1977)

Abstract—A finite strip method is presented for calculating the linear buckling stresses of structural assemblies of long, thin plate components which, in general, are curved and which are rigidly joined together at their longitudinal edges. It is assumed that on buckling under the action of a biaxial direct stress field the perturbation forces and displacements all vary sinusoidally in the longitudinal direction. A stiffness matrix relating the amplitudes of the perturbation forces and displacements is developed for the curved strip on the further assumption of relatively high-order polynomial variations of the displacement components around the plate width. Numerical results are presented of the application of the curved strip in calculating the buckling stresses of plates, cylinders, panels and formed sections.

INTRODUCTION

Considerable interest has been evidenced in recent years in the linear buckling analysis of structural assemblies of long, thin plate components (both flat and curved) by what may be broadly referred to as finite strip methods. In such structural assemblies the component plates are rigidly connected together at their junction lines and the structure cross-section does not vary longitudinally; typical structures are flat and curved panels, with or without stiffeners, thin-walled columns and formed sections. The buckling mode of the assembly may be of a local type in which the junction lines between component plates can be assumed to remain fixed and perfectly straight, or of an overall or torsional type where the wavelength is longer and where considerable movement of the junction lines is involved.

Wittrick[1, 2] laid the foundations of what could be termed an "exact" finite strip (i.e. exact within the limitations of linear theory) by developing a stiffness matrix for a long, flat plate strip subjected to a basic state of membrane stress which is longitudinally invariant; this basic stress state incorporates uniform longitudinal, transverse and shear stresses. It is assumed that when buckling occurs, in whatever type of mode, the three components of displacement vary sinusoidally in the longitudinal direction with a common wavelength. This assumption, which is universally adopted in all the related work referred to below, implies either that the buckled half-wavelength is small compared to the length of the plate assembly or that all the component plates are supported at their ends by a diaphragm (i.e. the plates are simply-supported so far as transverse displacement is concerned, are constrained against tangential in-plane displacement, but are allowed free movement in the axial direction). The assumption means that the problem is governed by ordinary differential equations which can be solved explicitly to yield stiffness matrices relating the amplitudes of the sinusoidally-varying forces and displacements† on the longitudinal edges of the plate strips. Each edge has four degrees of freedom comprising the three displacement components plus a rotation. Where shear stress is present the perturbation forces and displacements at the plate edges are generally out of phase and this is accounted for by specifying their magnitudes in terms of complex quantities; the stiffness matrix is then correspondingly complex and Hermitian. Whether or not shear is present the overall stiffness matrix for the plate assemblies in the "exact" finite strip method has components which are complicated transcendental functions of a loading factor and the half wave-length of the buckled mode. Standard eigenvalue methods can therefore not be used to find the critical values of loading factor. To overcome this difficulty an algorithm has been developed[3] but this requires the specification of an upper bound for the structure buckling load when all inter-strip junction lines are fully clamped.

†The words "forces" and "displacements" are, where appropriate, to be understood to be used in the general sense of including moments and rotations respectively.

Extensions of the early work of Wittrick have been made to encompass, amongst other things, anisotropy of the component flat plates, off-setting of component plates and sub-structuring; these developments are described in [4] where computational details are also given. "Exact" analyses having much in common with that of Wittrick for flat plate assemblies have been presented by Viswanathan *et al.*[5] and by Smith[6]; some comparison of the major differences in the associated computer programmes is available[4].

Visanathan *et al.*[7, 8] have proceeded to include curved anisotropic plates in their analysis. These plates have constant transverse curvature and thickness and can be subjected to uniform biaxial direct stress plus a uniform shear stress. The analysis is again exact in the sense that the chosen displacement function for each plate strip represents an exact solution, although in forming a strip stiffness matrix a numerical solution is required to find the roots of a polynomial equation. Of course, the resulting overall stiffness matrix is such that again standard eigenvalue routines cannot be used and the algorithm of [3] is needed to calculate the buckling loads. An alternative philosophy in dealing with plates of curved cross-section has been adopted by Williams[9, 10] who described buckling applications in which curved plates are idealised by assemblages of "exact" flat strips. Whilst this procedure appears feasible for curved plates carrying longitudinal stress, it is perhaps of questionable validity in some situations where such plates are subjected to transverse or shear stress. The procedure requires the employment of a large number of flat strips to model a curved geometry[9, 10], though the use of substructures can partly offset the resulting increase in computation.

In addition to the "exact" finite strips described above some application of the approximate finite strip method—which was introduced initially in the solution of static plate bending problems by Cheung[11]—has been made to the buckling problem. Przemieniecki[12] used the method to calculate the initial buckling stresses of assemblies of flat plates, each of which may be subjected to a basic biaxial stress system. However, the analysis assumes that all line junctions between component flats remain straight during buckling, i.e. only local buckling modes are included and only the displacement normal to any strip need be considered. The approximate method requires the assumption of the variation of the displacement components across the strip; in [12] it is assumed that the normal displacement varies as a cubic polynomial across the strip width. Plank and Wittrick[13] have extended this approach by removing the restriction to local modes of buckling and by admitting a more general state of stress which includes a uniform shear stress. The two membrane components of displacement are assumed to vary linearly across the width of a component flat plate and the complete degrees of freedom are the values at the strip edges of the three displacement components and a rotation, as in the "exact" strip. Again in common with the "exact" approach, if shear is present the phase differences between displacements and forces gives rise to stiffness matrices that are complex and Hermitian. Plank[14] has attempted to extend this work to curved plate strips by making similar assumptions for the variation of the displacements but this has not met with any success for reasons discussed in the next section.

As the name implies, the advantage of the "exact" approach is that, in circumstances where it can be applied and within the context of linear theory, the calculated buckling stress for an assembly of long, thin plates is the correct one when a single strip is used to model each component plate. Use of the approximate finite strip method often requires more than a single strip to model a component plate, with consequent increase in the size and bandwidth of the overall matrices. On the other hand there are advantages in using the approximate approach. One advantage, already mentioned, is that the terms of the total stiffness matrix are linear functions of a load factor and hence standard eigenvalue routines can be used to calculate the critical load levels. Another, and perhaps more important, advantage is that the approximate finite strip approach is potentially more generally applicable than is the "exact" approach. In principle, completely arbitrary geometry of cross-section can be accommodated and complicated variations across a strip of longitudinal stress can be incorporated (together with anisotropic material behaviour). Furthermore, the restriction to simply supported ends might possibly be removed and longitudinal variations of displacement appropriate to other end conditions be considered.

The present paper describes an approximate finite strip analysis of assemblies of rigidly-connected component strips which, in general, have transverse curvature. In this work the strip

material is isotropic and each strip is of uniform thickness and uniform curvature. A strip may be subjected to a uniform transverse stress and a non-uniform longitudinal stress; no shear stress is currently included and so no complex quantities arise. The curved strip has a total of sixteen degrees of freedom, being based on a comparatively high-order assumed displacement field incorporating quintic polynomial representations of the normal and circumferential components and a cubic representation of the axial component. A number of typical buckling problems are examined using the refined strip. In a concurrent investigation the strip has been applied to the solution of some cylindrical shell static problems by assuming that the variations of the displacement components in the longitudinal direction are given by trigonometric series[15].

Finally it is emphasised that the approach described here is a linear buckling one; no account is taken of any pre-buckling deformation or any geometrical imperfection so that the prescribed basic stress field is that existing in the perfect structure at the onset of buckling. As is well known, for curved shell structures the actual collapse loads do not always compare closely with the buckling loads calculated using linear buckling theory though, even when this is so, a knowledge of the linear buckling levels is useful. Within the context of the linear approach no restrictions are applied here on the possible mode of buckling.

THE CURVED STRIP AND ITS DISPLACEMENTS

The structure to be analysed is, in general, assembled from curved strips of the type shown in Fig. 1. The strip has a uniform radius of curvature R, a curved breadth $2B$ and is of uniform thickness h. At the onset of buckling the basic membrane stress system in the individual strip consists of a uniform transverse compressive stress σ_2 and a longitudinal compressive stress σ_1 whose intensity varies around the strip circumference. With the approximate finite strip method detailed here, there is no great difficulty in incorporating a complicated distribution of the longitudinal stress into the analysis and allowance is made for up to a quintic distribution around the strip.

The accuracy achieved in using the finite element (or strip) displacement method is directly dependent on the suitability of the initially assumed displacement field and this is particularly so in analysing thin curved structures. The present work is concerned with developing the properties of the circular cylindrical shell strip in terms of the system of tangential and normal displacement components u, v and w (i.e. the "surface" displacement components) that arise at buckling. The longitudinal variation of these displacement components is a sinusoidal one, with the displacement boundary conditions at the curved ends such that v and w are zero. This being so it remains to select the variation of each of the components in the circumferential direction only.

Some guidance in making the choice of the circumferential variations is available from related finite element studies by the author of the efficiency of various elements in the solution of static arch and shell problems[16–19]. The most direct approach—which is the one adopted here but which is not the only possibility—is to assume variations for the surface displacement components which are uncoupled polynomials in the circumferential coordinate. Then the previous studies clearly show that the efficiency of elements having a quintic variation of v and w is high, giving very good results for a wide range of geometries. Arch elements based

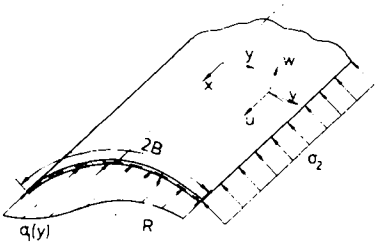

Fig. 1. Curved strip geometry and basic stress system.

on assumed polynomials for v and w of lower than quintic order are markedly less efficient than the quintic models[16, 17, 20]. This particularly applies to arch models in which the assumed displacement field is the simplest possible one with v and w as independently-interpolated polynomials of linear and cubic order respectively; convergence is very slow indeed for such a model. The basis for the selection of the axial displacement component u is not so clearly established but it is assumed in the present work that this component is somewhat less critical than the v and w components and can therefore be approximated with a lower-order (namely cubic) polynomial. This assumption is a convenient one (allowing the specification of an equal number of degrees of freedom at each of four axial lines, as described below) but the possibility that it would be more efficient to base the curved strip properties on a quintic assumption for u as well as for v and w is noted.

In Plank's buckling analysis[14] the circumferential variations of the membrane and normal components of displacement of a curved strip are taken to be linear and cubic polynomials and this low level of interpolation almost certainly accounts for the failure of the analysis. No numerical results are recorded using this simple curved model but lack of convergence is evidenced by checking the components of the total stiffness matrix of a curved plate as the plate is successively represented by an increasing number of strips.

In view of the above remarks the displacement components of the present curved strip at buckling are assumed to have the form

$$\begin{aligned} u &= \cos kx(b_1 + b_2 y + b_3 y^2 + b_4 y^3) \\ v &= \sin kx(b_5 + b_6 y + b_7 y^2 + b_8 y^3 + b_9 y^4 + b_{10} y^5) \\ \text{and } w &= \sin kx(b_{11} + b_{12} y + b_{13} y^2 + b_{14} y^3 + b_{15} y^4 + b_{16} y^5) \end{aligned} \tag{1}$$

where $k = \pi/\lambda$ and λ is the half-wavelength of the buckled structure.

A condition usually considered in the selection of displacement fields in the finite element method is that of precisely representing, or at least closely approximating, the rigid-body motions of an element. It is noted in using the finite strip method, as here, that a true rigid-body motion cannot possibly occur (since, from eqn (1), all strips are held against v and w displacement at the ends $x = 0$ and $x = \lambda$ and are held against u displacement at $x = \lambda/2$), though it is possible for a cross-section to be displaced in its plane with little or no distortion. The comparatively high order of the assumed displacement field of eqn (1) will help to closely represent movements involving either small or large distortion of the cross-section.

The displacement field of eqn (1) includes sixteen coefficients, b_i, $i = 1 \ldots 16$, which have to be related to the sixteen degrees of freedom of the curved strip. The degrees of freedom selected here for the individual strip are located at four reference lines in the arrangement shown in Fig. 2. Note that the freedoms at the outside lines are only those strictly necessary to meet the compatibility requirements at the strip boundaries, i.e. they are the amplitudes of the three displacement components and the rotation ϕ where

$$\phi = \frac{\partial w}{\partial y} - \frac{v}{R}. \tag{2}$$

BUCKLING ANALYSIS

On buckling of the structure the perturbation displacement field of the curved strip, eqn (1), can be expressed in matrix notation as

$$\begin{Bmatrix} u \\ v \\ w \end{Bmatrix} = \begin{bmatrix} \cos kx & 0 & 0 \\ 0 & \sin kx & 0 \\ 0 & 0 & \sin kx \end{bmatrix} \left[\begin{array}{c|c|c} 1, y, y^2, y^3 & \mathbf{0} & \mathbf{0} \\ \hline \mathbf{0} & 1, y, y^2, y^3, y^4, y^5 & \mathbf{0} \\ \hline \mathbf{0} & \mathbf{0} & 1, y, y^2, y^3, y^4, y^5 \end{array}\right] \begin{Bmatrix} b_1 \\ b_2 \\ \vdots \\ b_{16} \end{Bmatrix}$$

$$= \mathbf{S}\,\mathbf{A}\mathbf{b}. \tag{3}$$

The coefficients b_i ($i = 1,2 \ldots 16$) are related to the strip degrees of freedom (i.e. the amplitudes

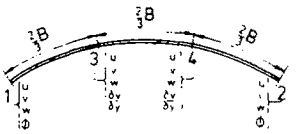

Fig. 2. The degrees of freedom of the single strip.

of the displacements at the reference lines) by the equation

$$\mathbf{b} = \mathbf{C}\,\mathbf{d}. \tag{4}$$

Here

$$\mathbf{d} = \{u_1, v_1, w_1, \phi_1, u_2, v_2, w_2, \phi_2, u_3, v_3, w_3, \theta_3, u_4, v_4, w_4, \theta_4,\} \tag{5}$$

where $\theta = \partial v/\partial y$, and $\mathbf{C}$ is a 16×16 matrix whose terms are constants for a particular strip geometry. Thus the perturbation displacement field can be written directly in terms of the displacement amplitudes as

$$\{u, v, w\} = \mathbf{S}\,\mathbf{A}\,\mathbf{C}\,\mathbf{d}. \tag{6}$$

Over the wavelength 2λ the displacements along the reference lines themselves are

$$\mathbf{d}^* = \mathbf{r}\,\mathbf{d} \tag{7}$$

where $\mathbf{r}$ is a 16×16 diagonal matrix defined by

$$\mathbf{r} = [\cos kx, \sin kx, \sin kx, \sin kx, \cos kx \ldots\ldots \sin kx]. \tag{8}$$

Corresponding to the perturbation displacements, at buckling the strip is subjected to a system of perturbation forces at the reference lines which are also distributed sinusoidally in the longitudinal direction with a half-wavelength λ. These perturbation forces can be represented as

$$\mathbf{F}^* = \mathbf{r}\,\mathbf{F} \tag{9}$$

where

$$\mathbf{F} = \{U_1, V_1, W_1, M_1, U_2, V_2, W_2, M_2, U_3, V_3, W_3, \Theta_3, U_4, V_4, W_4, \Theta_4,\} \tag{10}$$

is the vector of force amplitudes corresponding to the displacement amplitudes $\mathbf{d}$ of eqn (5).

Consider now the virtual work of the system produced during virtual displacements corresponding to a variation $\delta\mathbf{d}$ in the displacement (amplitude) vector $\mathbf{d}$.

The virtual work δW_e done by the distributed edge forces over the wavelength 2λ is, using eqns (7) and (9),

$$\delta W_e = \int_0^{2\lambda} \delta\mathbf{d}^{*T}.\,\mathbf{F}^*\,dx = \delta\mathbf{d}^T \left(\int_0^{2\lambda} \mathbf{r}\,.\,\mathbf{r}\,dx\right)\mathbf{F} \tag{11}$$

$$\text{and since} \int_0^{2\lambda} \sin^2 kx\,dx = \int_0^{2\lambda} \cos^2 kx\,dx = \lambda \tag{12}$$

this becomes

$$\delta W_e = \lambda\delta\mathbf{d}^T\,\mathbf{F}. \tag{13}$$

To calculate the internal virtual work over the wavelength of the strip, the shell theory of

Koiter[21] is used to express the linear median strains (ϵ_1, ϵ_2 and ϵ_{12}) and curvature changes (κ_1, κ_2 and κ_{12}) in terms of the displacement components as

$$\begin{Bmatrix} \epsilon_1 \\ \epsilon_2 \\ \epsilon_{12} \end{Bmatrix} = \boldsymbol{\xi} = \begin{Bmatrix} \dfrac{\partial u}{\partial x} \\ \dfrac{\partial v}{\partial y} + \dfrac{w}{R} \\ \dfrac{\partial v}{\partial x} + \dfrac{\partial u}{\partial y} \end{Bmatrix} \text{ and } \begin{Bmatrix} \kappa_1 \\ \kappa_2 \\ \kappa_{12} \end{Bmatrix} = \boldsymbol{\kappa} = \begin{Bmatrix} \dfrac{\partial^2 w}{\partial x^2} \\ \dfrac{\partial^2 w}{\partial y^2} - \dfrac{1}{R}\dfrac{\partial v}{\partial y} \\ \dfrac{\partial^2 w}{\partial x \partial y} + \dfrac{1}{4R}\dfrac{\partial u}{\partial y} - \dfrac{3}{4R}\dfrac{\partial v}{\partial x} \end{Bmatrix} \tag{14}$$

Using eqns (6) and (14) the median strains and curvatures can then be expressed in the form

$$\boldsymbol{\xi} = \mathbf{S}_1 \mathbf{G}_1 \mathbf{C}\,\mathbf{d} \text{ and } \boldsymbol{\kappa} = \mathbf{S}_2 \mathbf{G}_2 \mathbf{C}\,\mathbf{d}. \tag{15}$$

Here $\mathbf{S}_1$ and $\mathbf{S}_2$ are 3×3 diagonal matrices whose non-zero terms are functions of the x coordinate only whilst $\mathbf{G}_1$ and $\mathbf{G}_2$ are 3×16 rectangular matrices whose terms are functions of the y coordinate only. (These matrices are defined by eqns (18)–(21) of reference [15], with the suffix m in these equations ignored, and thus need not be listed here).
The stress resultants (N_1, N_2 and N_{12}) and couples (M_1, M_2 and M_{12}) are assumed to be expressible in the form

$$\{N_1, N_2, N_{12}\} = \mathbf{N} = \mathbf{H}_1 \boldsymbol{\xi} \quad \text{and} \quad \{M_1, M_2, 2M_{12}\} = \mathbf{M} = \mathbf{H}_2 \boldsymbol{\kappa}. \tag{16}$$

where the terms of 3×3 matrices $\mathbf{H}_1$ and $\mathbf{H}_2$ depend on the elastic properties of the strip material. The internal virtual work δW_i done over the wavelength 2λ due to the virtual displacement $\delta\mathbf{d}$ is

$$\delta W_i = \int_{-B}^{B} \int_0^{2\lambda} (\delta\boldsymbol{\xi}^T \mathbf{N} + \delta\boldsymbol{\kappa}^T \mathbf{M})\, dx\, dy. \tag{17}$$

Using eqns (15) and (16) and performing the integration with respect to x (see eqn (12)) allows δW_i to be written as

$$\delta W_i = \lambda\, \delta\mathbf{d}^T \mathbf{K}\, \mathbf{d} \tag{18}$$

where

$$\mathbf{K} = \mathbf{C}^T \left(\int_B^B \mathbf{G}_1{}^T \bar{\mathbf{H}}_1 \mathbf{G}_1 + \mathbf{G}_2{}^T \bar{\mathbf{H}}_2 \mathbf{G}_2\, dy \right) \mathbf{C}. \tag{19}$$

For an isotropic strip

$$\bar{\mathbf{H}}_1 = \frac{Eh}{(1-\nu^2)} \begin{bmatrix} 1 & \nu & 0 \\ \nu & 1 & 0 \\ 0 & 0 & \frac{1}{2}(1-\nu) \end{bmatrix} \text{ and } \bar{\mathbf{H}}_2 = \frac{Eh^3}{12(1-\nu^2)} \begin{bmatrix} 1 & \nu & 0 \\ \nu & 1 & 0 \\ 0 & 0 & 2(1-\nu) \end{bmatrix} \tag{20}$$

where E and ν are Young's modulus and Poisson's ratio.

The virtual work, W_s, done by the basic membrane stress system during the virtual displacement is

$$\delta W_s = h \int_{-B}^{B} \int_0^{2\lambda} \sigma_1(y) \delta\epsilon_{11}\, dx dy + h\sigma_2 \int_{-B}^{B} \int_0^{2\lambda} \delta\epsilon_{22}\, dx dy. \tag{21}$$

Here ϵ_{11} and ϵ_{22} are the second-order expressions for the strains given by

$$\epsilon_{11} = \tfrac{1}{2}\left[\left(\frac{\partial u}{\partial x}\right)^2 + \left(\frac{\partial v}{\partial x}\right)^2 + \left(\frac{\partial w}{\partial x}\right)^2\right] \tag{22}$$

and

$$\epsilon_{22} = \tfrac{1}{2}\left[\left(\frac{\partial u}{\partial y}\right)^2 + \left(\frac{\partial v}{\partial y} + \frac{w}{R}\right)^2 + \left(\frac{\partial w}{\partial y} - \frac{v}{R}\right)^2\right]. \tag{23}$$

In the analysis all terms in these expressions are retained although it could be argued that some of them, being proportional to the squares of strains, could be eliminated without sensibly affecting results.
Now

$$\int_0^{2\lambda} \delta\epsilon_{11}\,dx = \int_0^{2\lambda} \left(\frac{\partial u}{\partial x}\cdot\frac{\partial \delta u}{\partial x} + \frac{\partial v}{\partial x}\cdot\frac{\partial \delta v}{\partial x} + \frac{\partial w}{\partial x}\cdot\frac{\partial \delta w}{\partial x}\right) dx$$

$$= -\int_0^{2\lambda} \left(\delta u\frac{\partial^2 u}{\partial x^2} + \delta v\frac{\partial^2 v}{\partial x^2} + \delta w\frac{\partial^2 w}{\partial x^2}\right) dx. \tag{24}$$

on integrating by parts and applying the boundary conditions at $x = 0$ and $x = \lambda$. This allows δW_s to be expressed in the form

$$\delta W_s = -h\int_{-B}^{B} \sigma(y)\left(\int_0^{2\lambda} [\delta u, \delta v, \delta w]\begin{Bmatrix} \partial^2 u/\partial x^2 \\ \partial^2 v/\partial x^2 \\ \partial^2 w/\partial x^2 \end{Bmatrix} dx\right) dy$$

$$+ h\sigma_2 \int_{-B}^{B}\int_0^{2\lambda} \left([\delta u, \delta v, \delta w] \begin{Bmatrix} 0 \\ \frac{v}{R^2} - \frac{1}{R}\frac{\partial w}{\partial y} \\ \frac{w}{R^2} + \frac{1}{R}\frac{\partial v}{\partial y} \end{Bmatrix} + \frac{\partial}{\partial y}[\delta u, \delta v, \delta w] \begin{Bmatrix} \partial u/\partial y \\ \frac{\partial v}{\partial y} + \frac{w}{R} \\ \frac{\partial w}{\partial y} - \frac{v}{R} \end{Bmatrix} \right) dx\,dy. \tag{25}$$

On integrating with respect to x, using eqn (12), this can be put in the form

$$\delta W_s = \lambda \delta \mathbf{d}^T (\mathbf{L}_1 + \mathbf{L}_2)\,\mathbf{d} \tag{26}$$

where

$$\mathbf{L}_1 = h\frac{\pi^2}{\lambda^2}\mathbf{C}^T\left(\int_{-B}^{B} \sigma_1(y)\,\mathbf{A}^T\,\mathbf{A}\,dy\right)\mathbf{C} \tag{27}$$

and

$$\mathbf{L}_2 = h\sigma_2\mathbf{C}^T\left(\int_{-B}^{B}\left[\mathbf{A}^T\,\mathbf{T}_1 + \frac{\partial}{\partial y}(\mathbf{A}^T)\,\mathbf{T}_2\right] dy\right)\mathbf{C}. \tag{28}$$

The matrices $\mathbf{T}_1$ and $\mathbf{T}_2$ are defined as

$$\mathbf{T}_1 = \left[\begin{array}{c|c|c} \mathbf{0} & \mathbf{0} & \mathbf{0} \\ \hline \mathbf{0} & \frac{1}{R^2}(1,y,y^2,y^3,y^4,y^5) & -\frac{1}{R}(0,1,2y,3y^2,4y^3,5y^4) \\ \hline \mathbf{0} & \frac{1}{R}(0,1,2y,3y^2,4y^3,5y^4) & \frac{1}{R^2}(1,y,y^2,y^3,y^4,y^5) \end{array}\right] \tag{29}$$

and

$$\mathbf{T}_2 = \left[\begin{array}{c|c|c} 0,1,2y,3y^2 & \mathbf{0} & \mathbf{0} \\ \hline \mathbf{0} & 0,1,2y,3y^2,4y^3,5y^4 & \frac{1}{R}(1,y,y^2,y^3,y^4,y^5) \\ \hline \mathbf{0} & -\frac{1}{R}(1,y,y^2,y^3,y^4,y^5) & 0,1,2y,3y^2,4y^3,5y^4 \end{array}\right] \tag{30}$$

The principle of Virtual Work is now applied to give

$$\delta W_i = \delta W_e + \delta W_s \tag{31}$$

Substituting in from eqns. (13), (18) and (26) and noting that $\delta\mathbf{d}$ is arbitrary leads to

$$\mathbf{F} = (\mathbf{K} - [\mathbf{L}_1 + \mathbf{L}_2])\mathbf{d} = (\mathbf{K} - \mathbf{L}_{12})\,\mathbf{d}. \tag{32}$$

The three matrices $\mathbf{K}$, $\mathbf{L}_1$ and $\mathbf{L}_2$ are square matrices of order 16 and in the absence of an applied shear stress, all are real and symmetric. $\mathbf{K}$ is, of course, the linear elastic stiffness matrix of the strip whilst $\mathbf{L}_1$ and $\mathbf{L}_2$ are contributions to the total geometric stiffness matrix $\mathbf{L}_{12}$. The terms of $\mathbf{L}_1$ are directly proportional to the (non-uniform) intensity of the basic longitudinal stress whilst those of $\mathbf{L}_2$ are similarly proportional to the (uniform) intensity of the transverse stress. In many applications, including those detailed below, the components of the basic stress system are in a fixed ratio one to another and it is then a simple matter to express the geometric stiffness matrix in the form $\mathbf{L}_{12} = \sigma_s\mathbf{L}$ where σ_s is some typical specified stress component.

The structure stiffness etc. is obtained by summation of the element stiffnesses in the usual way, applying as necessary any required transformations to a common global displacement system (denoted by suffix g) and any displacement boundary conditions on the longitudinal edges. The overall stiffness equation then becomes

$$\mathbf{F}_g = (\mathbf{K}_g - \sigma_s\mathbf{L}_g)\mathbf{d}_g. \tag{33}$$

In the eigenvalue problem $\mathbf{F}_g = \mathbf{0}$ and therefore the stability equation is

$$\mathbf{K}_g\,\mathbf{d}_g = \sigma_s\mathbf{L}_g\mathbf{d}_g \tag{34}$$

which can be solved by standard eigenvalue methods to yield the critical values of the stress factor σ_s and the corresponding eigenvectors.

The terms of the elastic and geometric stiffness matrices are, of course, dependent on the half-wavelength of buckling. Those of $\mathbf{L}_1$ are proportional to λ^{-2}, of $\mathbf{L}_2$ to λ^0 and the individual terms of $\mathbf{K}$ in general contain components proportional to λ^{-4}, λ^{-2}, λ^{-1} and λ^0. The value of λ has to be supplied for each eigenvalue analysis but usually the true value of λ corresponding to the minimum buckling stress is not known initially. In these circumstances it is necessary to perform eigenvalue calculations at several appropriate assumed values of λ and thence to determine the minimum critical stress either graphically or by some other convenient means. For a plate structure of given overall length it will be known that the half-wavelength of buckling must be an integer fraction of the overall length.

NUMERICAL APPLICATIONS

The theory of the preceeding section has been incorporated into a computer programme for the calculation of the buckling stresses of assemblies of flat and curved strips. Calculations have been made in single length arithmetic (about eleven significant figures). In the applications reported below all degrees of freedom have been employed in full eigenvalue analyses, i.e. there has been no attempt to condense out in any way any of the degrees of freedom.

The results presented fall naturally into the three groupings of (a) flat plate problems, (b)

complete circular cylinder problems, and (c) general problems including curved panels and formed sections.

The flat plate problems are included so as to verify the present strip method in the limiting case of flat geometry, where comparative results are readily available, and to allow some comparison to the efficiency of the present strip with that of the lower order strip of Plank and Wittrick[13]. Group (b) problems test the strip in the other limiting condition of the full cylinder. The group (c) problems are more typical of the sort of applications envisaged for the curved strip, although there are insufficient available comparative results to fully indicate the scope of the method.

Unless otherwise stated the value of Poisson's ratio used in the examples is 0.3.

(a) *Flat plate structures*

Results for the out-of-plane buckling of single plates with the longitudinal edges either both simply-supported or both clamped are presented in Tables 1 and 2; the loadings are uniform longitudinal compression ($\sigma = \sigma_1$), uniform biaxial compression ($\sigma = \sigma_1 = \sigma_2$) or pure in-plane bending (with σ_b denoting the bending stress). The plates are of width b and the calculations are for values of wavelength corresponding to the exact or nearly-exact comparative buckling stresses. (The comparative results for the bending stress case are known to be slightly high). Results obtained using the present strip (with one or two strips in the complete plate) and the low-order strip[13] (with two or four strips in the complete plate) are compared on a degree-of-freedom basis. The results show the high accuracy of the present strip and indicate its increased efficiency, even in simple flat geometry situations, compared to the earlier strip; for curved geometry this increased efficiency would be expected to be more pronounced.

As an example of a more complicated problem the integrally stiffened flat panel of Fig. 3 is studied. The applied longitudinal stress is of uniform value σ_u in the main plate and varies linearly in the stiffeners from σ_u at the plate/stiffener junctions to zero at the free edges. The ratio b/h equals 50 and the two extreme longitudinal edges of the main plate are simply supported such that only vertical motion is prevented. In applying the finite strip method the whole of the plate is discretised, with a single strip used for each component plate. The "exact" solution for this problem[10], based on the theory of [1, 2], is that the critical value of σ_u is $1.787.10^{-3}$E with a corresponding longitudinal half-wavelength λ of 0.92 b. For this value of λ the present method in fact yields the exact value of the initial buckling stress (to the four-figure

Table 1. Buckling of flat plates in uniaxial and biaxial compression. Values of $b^2h\sigma/\pi^2D$

Simply supported edges				Clamped edges		
Final degrees of freedom	Uniaxial comp. ($\lambda/b = 1.0$) Present strip	Low-order strip[13]	Biaxial comp. ($\lambda/b = 1.0$) Present strip	Final degrees of freedom	Uniaxial comp. ($\lambda/b = 0.661$) Present strip	Low-order strip[13]
4	4.0007	4.0086	2.0003	2	6.9811	7.2261
8	4.0000	4.0005	2.0000	6	6.9714	6.9908
Exact results[22]	4.0000	4.0000	2.0000		6.9709	6.9709

Table 2 Buckling of flat plates in pure bending. Values of $b^2h\sigma_b/\pi^2D$

Simply supported edges ($\lambda/b = 0.667$)			Clamped edges ($\lambda/b = 0.47$)		
Final d.o.f.	Present strip	Low-order strip[13]	Final d.o.f.	Present strip	Low-order strip[13]
4	24.363	25.454	2	44.703	49.760
8	23.886	23.965	6	39.567	40.361
Comparative results[23]	23.9	23.9		39.6	39.6

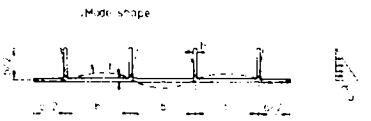

Fig. 3. Details of integrally stiffened flat panel.

accuracy that the exact result is quoted). The buckled mode is a local one, as indicated in Fig. 3.

(b) *Complete cylinders*

The first problem considered is the well-known one of the thin circular cylinder under uniform axial compression. For this problem the classical results of Flügge[24] are available whilst recently Dym[25] has used the more-refined shell theory of Budiansky and Koiter[26, 27] to calculate detailed results which are compared with those of Flügge for a particular shell geometry and particular modes of buckling. The calculated finite strip buckling stresses for this problem together with the comparative results given by Dym are presented in Table 3. The buckling stresses correspond to specified numbers, n, of circumferential waves and to four different values of longitudinal half-wavelength. The finite strip results are obtained by analysing a quarter of the cylinder with applied boundary conditions at the longitudinal boundaries which are appropriate to the mode under consideration, i.e. v and ϕ zero at both boundaries for even modes, v and ϕ zero at one edge and u and w zero at the other for odd modes. Generally the finite strip results show rapid convergence and compare very well with those of Dym, except in the case of the mode $n = 0$ with λ/R values of 10 and 90; it is for these long wavelength axisymmetric modes that the only major discrepancy between Dym's and Flügge's results occurs. The curved finite strip represents the axisymmetric mode exactly and it is not clear why the results of [25] differ from the present results in these cases. In practical terms the discrepancy is not important since for these wavelengths there are several critical levels of stress of lower magnitude than that corresponding to $n = 0$.

Simitses and Aswani[28] have documented results for the buckling of thin cylinders under a pressure-type loading. They have considered two cases of load behaviour during buckling; one of these corresponds to the existence of a state of uniform transverse stress σ_2 in the cylinder throughout buckling and it is this case which is considered here. The calculated buckling

Table 3. Buckling of axially-loaded complete cylinder. Values of $(\sigma_1(1-\nu^2)/E)$ for $(h/R)^2 = 12.10^{-4}$

		Comparative results[25]		Finite strip results		
		Flügge	Dym "Exact"	No. of strips in quadrant		
n	$\frac{\lambda}{R}$	Theory	Theory	1	2	3
	0.1	0.01078	0.01079	0.01079	0.01079	0.01079
0	1	0.09229	0.09138	0.09138	0.09138	0.09138
	10	9.22022	0.35001	0.90121	0.90121	0.90121
	90	746.838	0.35001	0.90990	0.90990	0.90990
	0.1	0.01080	0.01081	0.01081	0.01081	0.01081
1	1	0.07549	0.07244	0.07244	0.07244	0.07244
	10	0.04609	0.03539	0.03541	0.03539	0.03539
	90	0.00055	0.00055	0.0005773	0.0005529	0.0005526
	0.1	0.01086	0.01086	0.01086	0.01086	0.01086
	1	0.04591	0.04324	0.04325	0.04325	0.04325
2	10	0.00510	0.00501	0.005053	0.005017	0.005009
	90	0.05919	0.05917	0.06049	0.05919	0.05918
	0.1	0.01095	0.01095	0.01095	0.01095	0.01095
3	1	0.02492	0.02373	0.02375	0.02374	0.02373
	10	0.00696	0.00693	0.009405	0.006982	0.006935
	90	0.47289	0.47284	0.50775	0.47315	0.47285
	0.1	0.01108	0.01108	0.01109	0.01108	0.01108
4	1	0.01372	0.01327	0.01426	0.01328	0.01328
	10	0.02207	0.02204	0.03136	0.02214	0.02205
	90	1.7382	1.7382	1.8970	1.7461	1.7383

stresses of [28] are based on different types of shell equations including those of Budiansky–Koiter [26, 27] and Sanders [29]. These results, for a particular shell geometry with $R/h = 35$, are shown in Table 4 together with corresponding finite strip values obtained again by analysing a quarter of the cylinder. The finite strip results, based on the use of three strips, compare closely with both sets of comparative results. The slight discrepancies between the sets of results reflect the differences in the shell equations used.

An example of the buckling of a complete circular cylinder under nonuniform axial compression is provided by Flügge [24] and is illustrated in Fig. 4. The nonuniform axial force per unit length of circumference is defined by

$$N = P_0 + P_1 \cos \beta$$

and this can be very closely represented by the permitted quintic variation of axial stress within each finite strip. For a shell with $l/R = \pi$, $(h/R)^2 = 12.10^{-6}$ and $\nu = 1/6$ Flügge's approximate series solution for P_0/P_1 in the ratio 8/16.7 predicts initial buckling of the cylinder at a stress $\sigma_0 = P_0/h = 8.10^{-4}E/(1-\nu^2)$. The mode of buckling has one half-wave along the cylinder length and is symmetric about the vertical centre line of the cylinder. The finite strip solutions for this problem are given in Table 5 and correspond to the use of up to six strips in the half cylinder. The strip assemblies in this application are graded toward the top of the cylinder where the most complicated behaviour occurs. (Measured from the top centre the strips used in the 3, 4 and 6-strip assemblies subtend angles of 40, 60 and 80; 25, 35, 50 and 70; 12, 20, 25, 33, 40 and 50 degrees respectively). The finite strip results are converging on a buckling stress level which is only slightly different from that calculated in [24]. The associated buckling mode calculated by the present method is shown in Fig. 4 and is of the form predicted by Flügge.

(c) *Curved panels and formed sections*

Results for the buckling of cylindrical panels carrying a uniform axial stress σ_1 are available through the work of Chu and Krishnamoorthy [30]. In their work the longitudinal edges of the panel are completely free and the analysis is based on the approximate Donnell theory. Here,

Table 4 Buckling of complete cylinder under transverse stress. Values of $\sigma_2 R^2 h/D$ for $h/R = 1/35$

$\frac{l}{\pi}\frac{\lambda}{R}$	n	Comparative results [28] Budiansky -Koiter equations	Saunders equations	Finite strip results No. of strips in quadrant 1	2	3
1/3	6	72.259	72.433	115.643	73.278	72.169
1	4	21.363	21.461	28.980	21.367	21.357
3	2	8.5362	8.6121	8.5919	8.5297	8.5225
9	2	4.0812	4.0618	4.1269	4.0791	4.0781
15	2	4.0165	4.0157	4.0618	4.0156	4.0152
100	2	4.0000	4.0000	4.0456	4.0003	4.0002

Table 5 Buckling of complete cylinder under nonuniform axial compression. Value of $(\sigma_0(1-\nu^2).10^4/8E)$ for $(h/R)^2 = 12.10^{-6}$

No. of strips in half-cylinder	Calculated value
3	1.263
4	1.033
6	0.998
comparative solution [24]	1.000

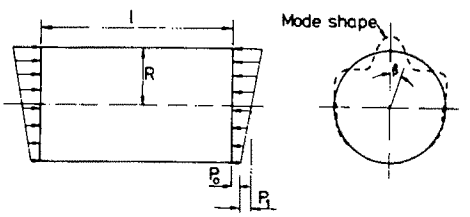

Fig. 4. Details of cylinder under non-uniform axial compression.

two particular panel cross-sections are considered, both subtending a central angle of 60 degrees but with h/R having the values 0.001 and 0.015 in turn. Poisson's ratio is 0.0. The finite strip results are shown together with the earlier results[30] in Fig. 5 as curves of buckling stress against longitudinal half-wavelength (or, since the lowest critical stress corresponds to a single longitudinal half-wave, against panel length). The strip results shown are based on the use of three equal strips in a half of the panel but it is noted that corresponding two-strip solutions are virtually coincident with the three-strip ones except for the thinner panel with $\lambda/R < 1$, approximately, where the buckled mode becomes progressively more complicated and difficult to model. Agreement between the present 3-strip results and those of Chu and Krishnamoorthy, based on Donnell theory, is good.

The buckling of four "advanced" structural panels has been considered by Viswanathan and Tamekuni[7] who present graphical results of the variation of the longitudinal buckling stress with half-wavelength. The geometry of the panels is shown in Fig. 6 where each given section represents a portion of a wider panel and antisymmetric boundary conditions (u and w zero) are applied at both outside edges of the given portion. The present strip results for these panels are illustrated in Fig. 7 together with point values obtained from the earlier graphs[7]; the typical mode shape is shown inset. The "finite strip A" results correspond to the use of curved strips subtending an angle $\alpha/2$ (with each of the flat parts of panels 1 and 2 represented by a single strip) whilst "finite strip B" results (calculated for panels 3 and 4 only) are related to each curved strip subtending an angle α. Close agreement of the "A" results with the results of Viswanathan and Tamekuni is apparent whilst the "B" results are around four per cent high. (These panels have also been analysed using the BOSOR3 code[31] and the results are given in [7]. BOSOR3 predicts buckling stresses of the order ten per cent higher than those calculated using the present method—"A" results—or the "exact" method).

The buckling under axial stress σ_1 of the pear-shaped cylinder shown in Fig. 8(a) has been studied by Bushnell[32] who found, in a linear analysis using the BOSOR3 computer code[31], that the lowest two buckling modes correspond, in turn, to buckling of the flat plate regions AB and CD, with a single half-wave in the axial direction. The analysis is based on the finite difference method used in conjuction with energy minimisation and treats cylinders as portions of very slender toriods. In using the finite strip method a symmetric half of the cylinder is analysed with four different levels of refinement corresponding to the use of 4 strips (one for

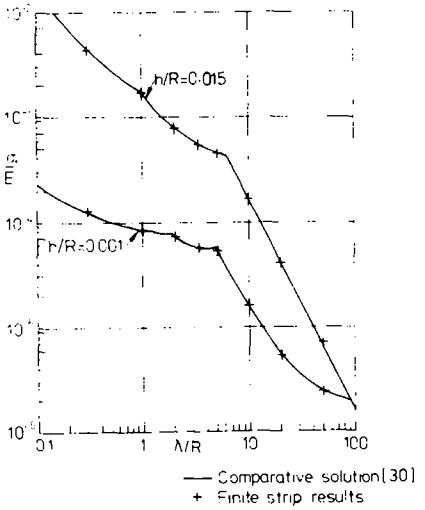

Fig. 5. Curves of σ_1/E versus λ/R for the free-edged panels.

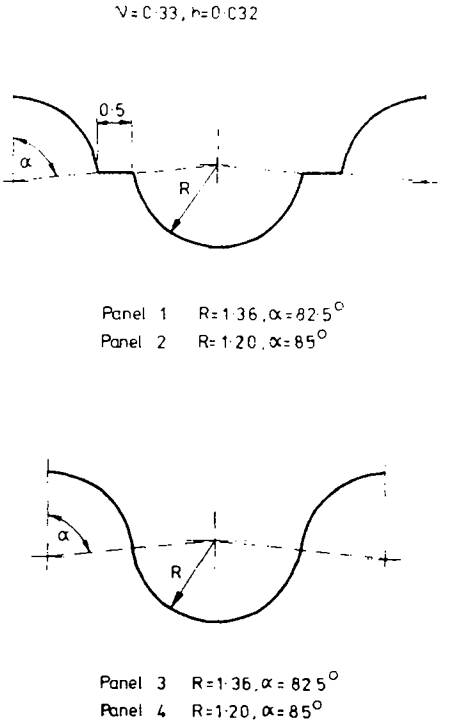

Fig. 6. Advanced structural panels: geometry.

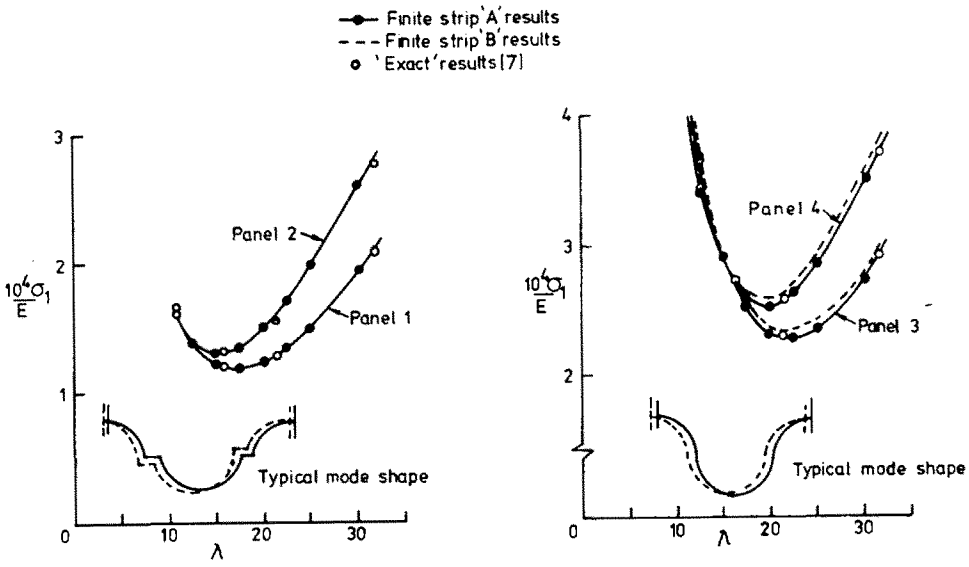

Fig. 7. Advanced structural panels: results.

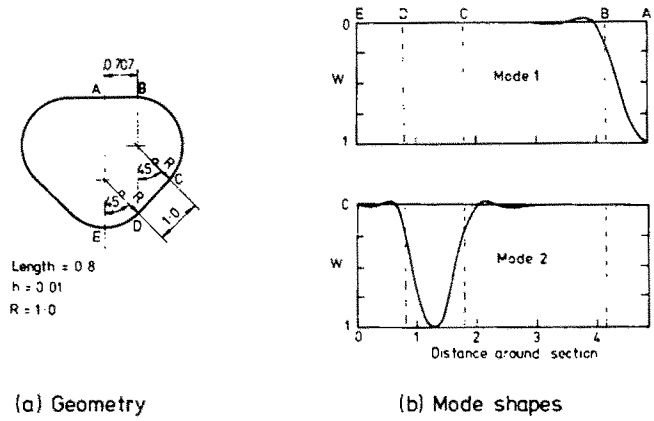

Fig. 8. Details of pear-shaped cylinder.

each flat or curved region of the half cylinder), 5 strips (two strips in region *BC*), 6 strips (3 in *BC*) and 8 strips (as the 6-strip assembly but with an extra strip in each of the flats *AB* and *CD*). Results for the lowest two buckling stresses are detailed in Table 6 where it appears that the finite strip results have converged on values a little higher than those forecast by Bushnell. Fig. 8(b) illustrates the mode shapes corresponding to the two lowest eigenvalues.

Viswanathan and Tamekuni[7] have investigated the buckling under uniform longitudinal compression σ_1 of the formed Z section shown in Fig. 9 using their "exact" method. The length of the strut is 3.0. Using the present method each component plate (flat or curved) is represented by a single finite strip (9 strips in all). A direct comparison of the results of the present analysis and the earlier results is given in Table 7 in the form of buckling stresses corresponding to 2, 3 or 4 longitudinal half-waves (the minimum buckling stress being associated with the mode having 3 half-waves). The present results compare closely with those of[7], being around 0.4% high in each case. The typical buckled mode shape in the plane of the cross-section is shown in Fig. 9. Finally it is noted that solutions to this particular problem have also been obtained by representing the section with assemblies of "exact" flat strips only. Plank and Williams[10] have idealised each curved portion of the section by an n-sided part of a regular polygon, with $n = 1$, 2, 4, 8, 16 or 32 in turn. Their results for $n = 8$ almost exactly coincide with those given in Table 7 for the present method, the latter obtained using one refined curved strip per curved portion.

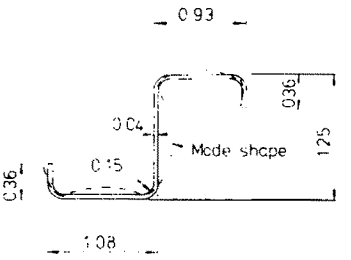

Fig. 9. Details of formed Z section.

Table 6 Buckling of pear-shaped cylinder

No. of strips	Values of $10^5\sigma_1/E$ First mode	Second mode
4	27.57	40.17
5	24.41	35.74
6	24.27	35.54
8	24.27	35.51
Comparative solutions[32]	24.02	34.74

Table 7 Buckling of Z section

No. of longitudinal half waves	Values of $10^3\sigma_1/E$ Present method	Reference[7]
2	6.071	6.049
3	5.765	5.741
4	6.465	6.437

CONCLUSIONS

An approximate finite strip linear buckling analysis for curved plate assemblies has been presented and has been verified in numerical applications. In the applications the particular curved strip described here has been shown to be an efficient one although, due to the scarcity of comparative results, the range of application considered does not fully reflect the scope of the method.

The analysis could be extended to include both anisotropic material behaviour and the presence of a uniform shear stress additional to the basic biaxial stress system considered here. Furthermore the method need not be limited to cross-sectional geometries in which the component plates have a uniform curvature and thickness, and the possibility also exists of dealing with end conditions other than simple supports.

Acknowledgements—The author wishes to record his gratitude to Professor W. H. Wittrick, Beale Professor of Civil Engineering at Birmingham University, both for initially suggesting this problem and for his encouragement during the period of the investigation.

REFERENCES

1. W. H. Wittrick, A unified approach to the initial buckling of stiffened panels in compression. *Aeronautical Quart.* **19**, 265 (1968).
2. W. H. Wittrick, General sinusoidal stiffness matrices for buckling and vibration analyses of thin flat-walled structures. *Int. J. Mech. Sci.* **10**, 949 (1968).
3. W. H. Wittrick and F. W. Williams, A general algorithm for computing natural frequencies of elastic structures. *Quart. J. Mech. App. Math.* **24**, 263 (1971).
4. W. H. Wittrick and F. W. Williams, Buckling and vibration of anisotropic or isotropic plate assemblies under combined loadings. *Int. J. Mech. Sci.* **16**, 209 (1974).
5. A. V. Viswanathan, T. C. Soong and R. E. Miller, Buckling analysis for axially compressed flat plates, structural sections and stiffened plates reinforced with laminated composites. *Int. J. Solids Structures* **8**, 347 (1972).
6. C. S. Smith, Bending, buckling and vibration of orthotropic plate-beam structures. *J. Ship Res.* **12**, 249 (1968).
7. A. V. Viswanathan and M. Tamekuni, Elastic buckling analysis for composite stiffened panels and other structures subjected to biaxial inplane loads. *NASA CR*-2216 (1973).
8. A. V. Viswanathan, M. Tamekuni and L. L. Baker, Elastic stability of laminated, flat and curved, long rectangular plates subjected to combined inplane loads. *NASA CR*-2330 (1974).
9. F. W. Williams, Approximations in complicated critical buckling and free vibration analyses of prismatic plate structures. *Aeronautical Quart.* **25**, 180 (1974).
10. R. J. Plank and F. W. Williams, Critical buckling of some stiffened panels in compression, shear and bending. *Aeronautical Quart.* **25**, 165 (1974).
11. Y. K. Cheung, The finite strip method in the analysis of elastic plates with two opposite simply supported ends. *Proc. Inst. Civil Engrs.*, **40**, 1 (1968).
12. J. S. Przemieniecki, Finite element structural analysis of local instability. *AIAA J.* **11**, 33 (1973).
13. R. J. Plank and W. H. Wittrick, Buckling under combined loading of thin, flat-walled structures by a complex finite strip method. *Int. J. Num. Meth. Engng* **8**, 323 (1974).

14. R. J. Plank, The initial buckling of thin walled structures under combined loadings. Ph.D. Thesis, University of Birmingham, England (1973).
15. D. J. Dawe, Static analysis of diaphragm-supported cylindrical shells using a curved finite strip. *Int. J. Num. Meth. Engng* (in press).
16. D. J. Dawe, Curved finite elements for the analysis of shallow and deep arches. *Computers and Structures* **4**, 559 (1974).
17. D. J. Dawe, Numerical studies using circular arch finite elements. *Computers and Structures* **4**, 729 (1974).
18. D. J. Dawe, High-order triangular finite element for shell analysis. *Int. J. Solids Structures* **11**, 1097 (1975).
19. D. J. Dawe, Some high-order elements for arches and shells. In *Finite Elements for Thin Shells and Curved Members* (Edited by D. G. Ashwell and R. H. Gallagher). Wiley, New York (1976).
20. D. G. Ashwell and A. B. Sabir, Limitations of certain curved finite elements when applied to arches. *Int. J. Mech. Sci.* **13**, 133 (1971).
21. W. T. Koiter, A consistent first approximation in the general theory of thin elastic shells. In *Theory of Thin Elastic Shells* (Edited by W. T. Koiter). North-Holland, Amsterdam (1960).
22. W. H. Wittrick and P. L. V. Curzon, Stability functions for the local buckling of thin flat-walled structures with the walls in combined shear and compression. *Aeronautical Quart.* **19**, 327 (1968).
23. F. Bleich, *Buckling Strength of Metal Structures*. McGraw-Hill, New York (1952).
24. W. Flügge, *Stresses in Shells*. Springer-Verlag, Berlin (1962).
25. C. L. Dym, On the buckling of cylinders in axial compression. *J. App. Mech.* **40**, 565 (1973).
26. B. Budiansky, Notes on nonlinear shell theory, *J. Appl. Mech.* **35**, 393 (1968).
27. W. T. Koiter, General equations of elastic stability for thin shells. In *Proc. Symp on the Theory of Shells* (Edited by D. Muster) University of Houston, Texas (1967).
28. G. T. Simitses and M. Aswani, Buckling of thin cylinders under uniform lateral loading. *J. Appl. Mech.* **41**, 827 (1974).
29. J. L. Sanders, Nonlinear theories of thin shells. *Quart. Appl. Math.* **21**, 21 (1963).
30. K. H. Chu and K. Krishnamoorthy, Buckling of open cylindrical shells. *Proc. ASCE* **96**, EM2, 177 (1967).
31. D. Bushnell, Stress, stability and vibration of complex shells of revolution: analysis and user's manual for BOSOR3. *SAMSO TR-69-375*. Lockheed Missiles and Space Co. (1969).
32. D. Bushnell, Stress, buckling and vibration of prismatic shells. *AIAA J.* **9**, 2004 (1971).